Electronic Supplementary Material (ESI) for Physical Chemistry Chemical Physics.

Supplementary Information

Mobility and Solvation Structure of Hydroxyl Radical in a Water Nanodroplet: A Born-Oppenheimer Molecular Dynamics Study

Mohammad Hassan Hadizadeh,[‡] Lewen Yang,[‡] Guoyong Fang, Zongyang Qiu, Zhenyu Li*

Hefei National Laboratory of Physical Sciences at the Microscale, University of Science and Technology of China, Hefei, Anhui, 230026, China

Email: zyli@ustc.edu.cn

1. Definition of the air-water interface

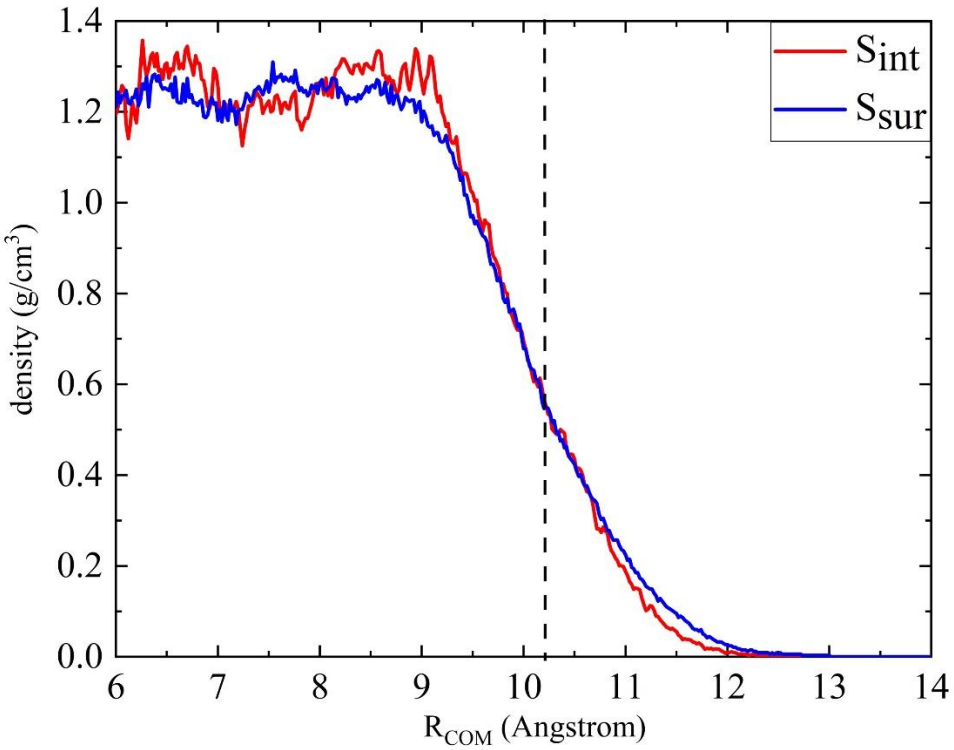

Fig. S1. Density profile of water molecules in the 191 H_2O nanodroplet with OH^* being initially placed in the interior region (red) and in the surface region (blue). The vertical dashed line located at 10.2 Å which corresponds to half of the bulk water density is defined as the air-water interface.

2. The deformation of water nanodroplet

Deformation (D) is defined as:

$$D = \frac{R_{max} - R_{min}}{R_{ave}}$$

where R_{max}, R_{min}, and R_{ave} are the maximum, minimum, and average distances between the droplet center and surface water molecules. As shown in **Figure S2**, trajectory S_{sur} undergoes a larger deformation compared to trajectory S_{int}.

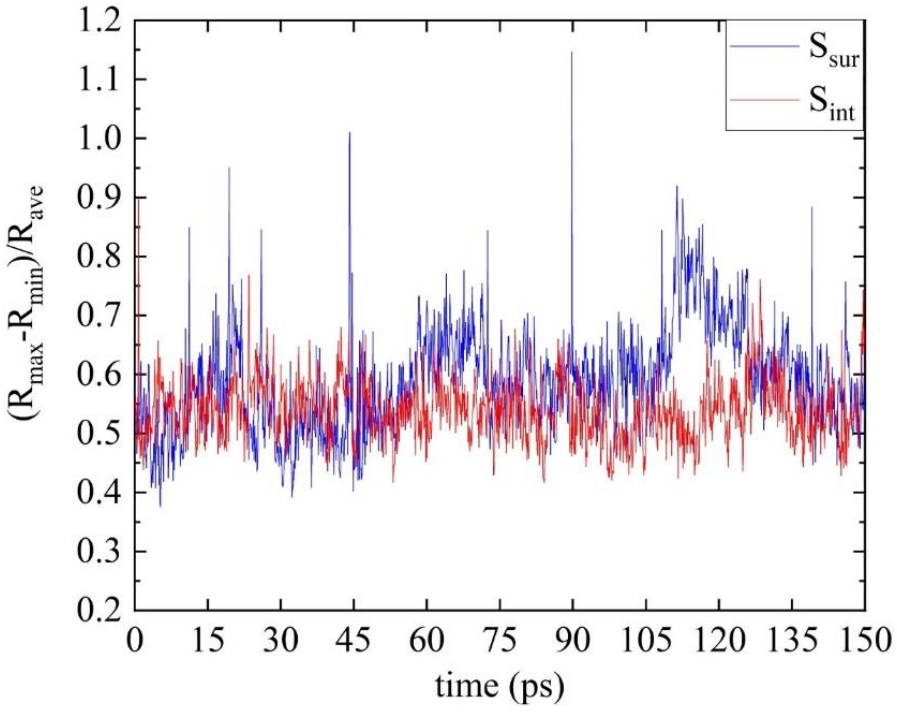

Fig. S2. The deformation of the water droplet *versus* simulation time for trajectory S_{sur} and S_{int}.

3. Atomic charges on the hydroxyl radical

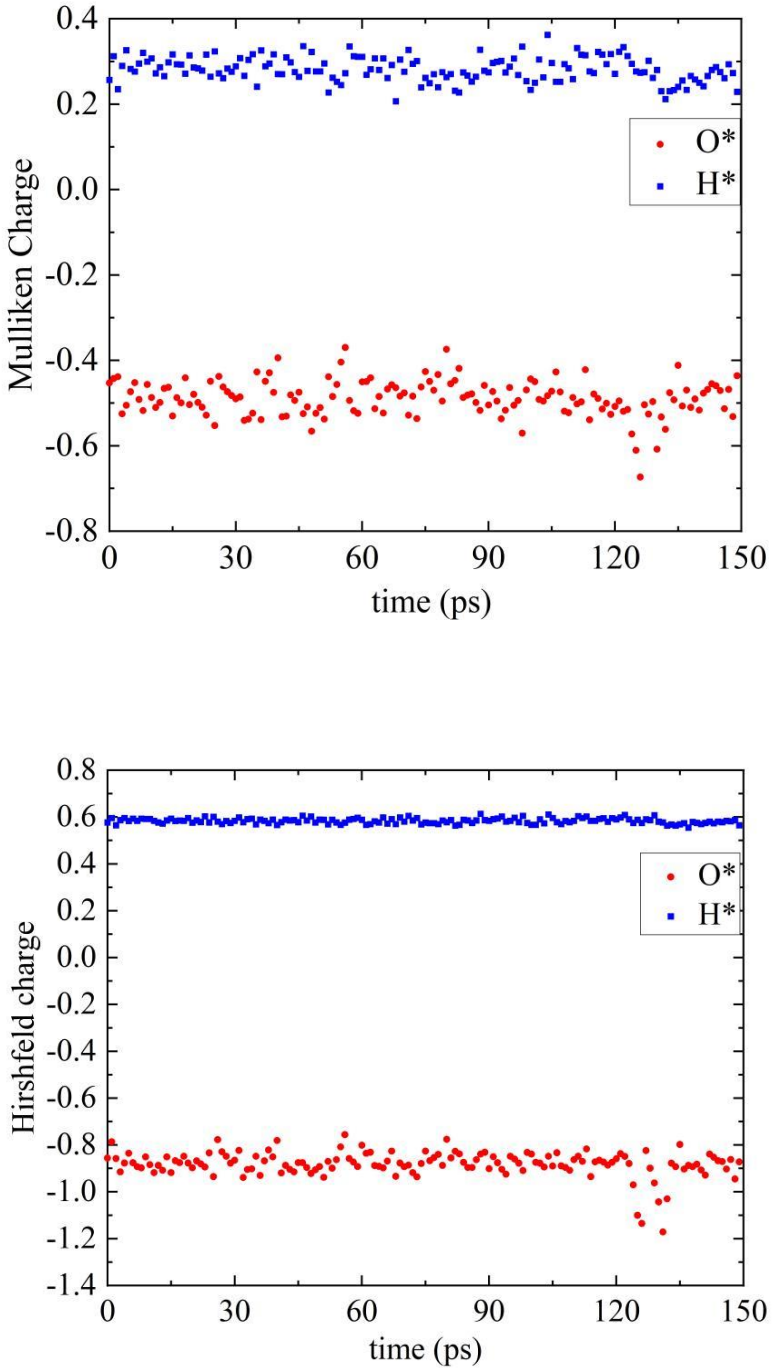

Fig. S3. The Mulliken and Hirshfeld charges of O^* and H^* in the hydroxyl radical.

4. Geometric criteria in defining hemibond

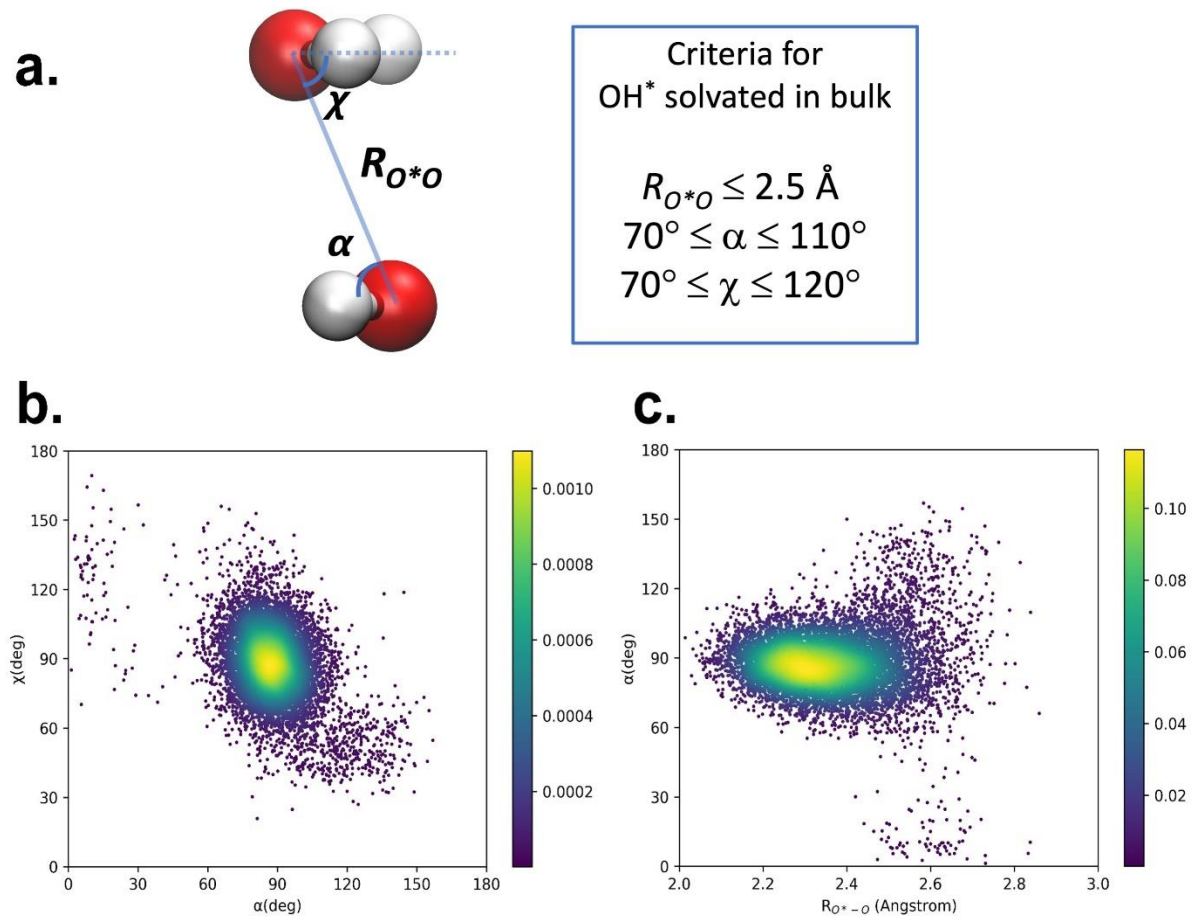

Fig. S4. (a) Schematic view of using the O*-O distance R_{O*O}, the OH* tilt angle α, and the O*-O azimuthal angle χ to define hemibonded structures. Geometric criteria for OH* in the bulk are taken from ref. 21 (see main text). (b) Joint probability distribution P(α, χ) and (c) Joint probability distribution P(R_{O*O}, α) computed for trajectory S_{int} from 30 ps to 125 ps. (Distribution plots for S_{sur} are very similar, which are not shown in here.)

5. $d_{O^*\text{-}O}$ *versus* time when simulated at the B3LYP-D3 level

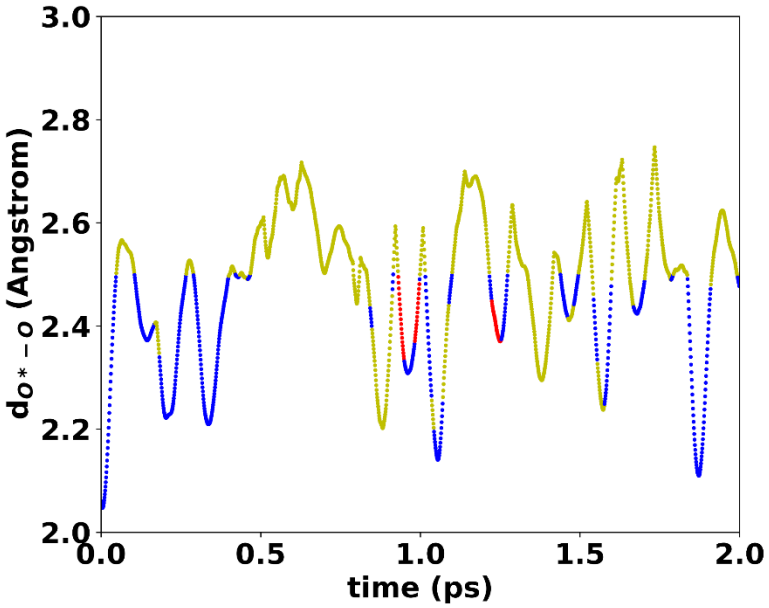

Fig. S5. The distance between O^* and its closest oxygen atom. Distances corresponding to hemibonded-configurations with one, two, and three H-atom donors to O^* are colored in green, blue, and red respectively. Distances corresponding to those without hemibond are colored in Kelly green.

6. Hydrogen bond statistics for OH^* complex at the surface

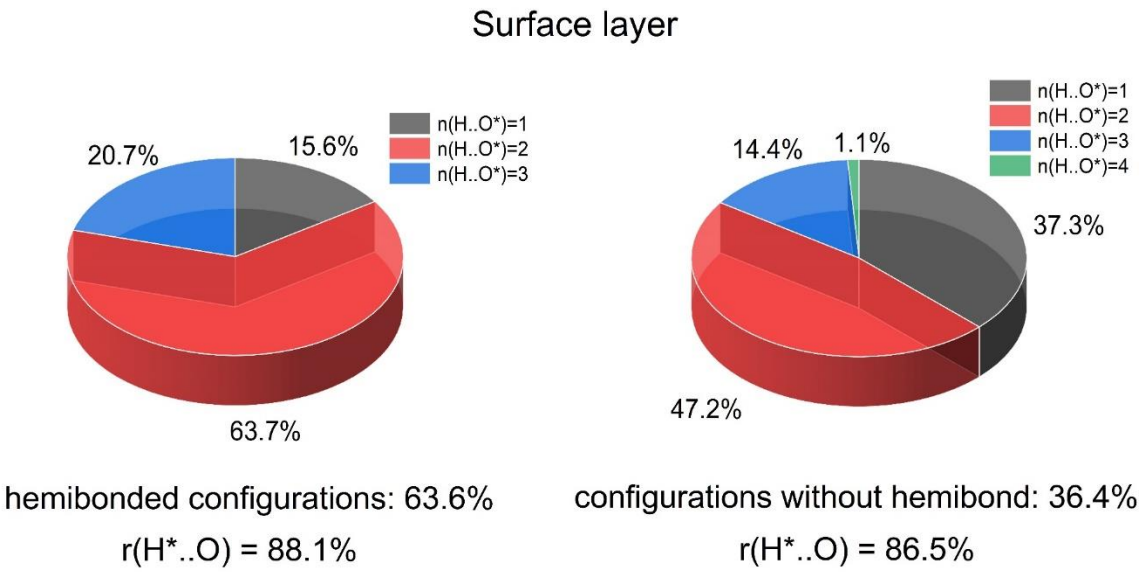

Fig. S6. The percentage of different numbers of hydrogen bonds connecting to O^* with (left) or without (right) a hemibond for trajectory S_{sur} from 0 to 30 ps. r(H^*..O) denotes the ratio of configurations where H^* forms a hydrogen bond with water oxygen.

7. $d_{O^*\text{-}O}$ *versus* time when simulated using TZVP basis

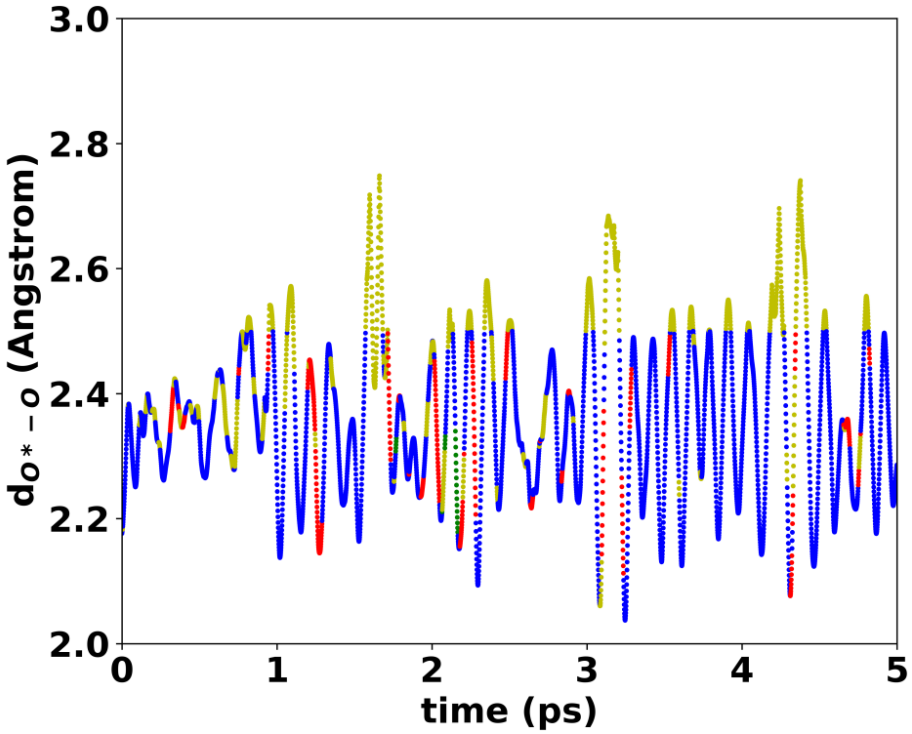

Fig. S7. The distance between O^* and its closest oxygen atom. Distances corresponding to hemibonded-configurations with one, two, and three H-atom donors to O^* are colored in green, blue, and red respectively. Distances corresponding to those without hemibond are colored in Kelly green.

8. *P*(θ, ϕ) for water oxygen atoms and water hydrogen atoms among hemibonded structures

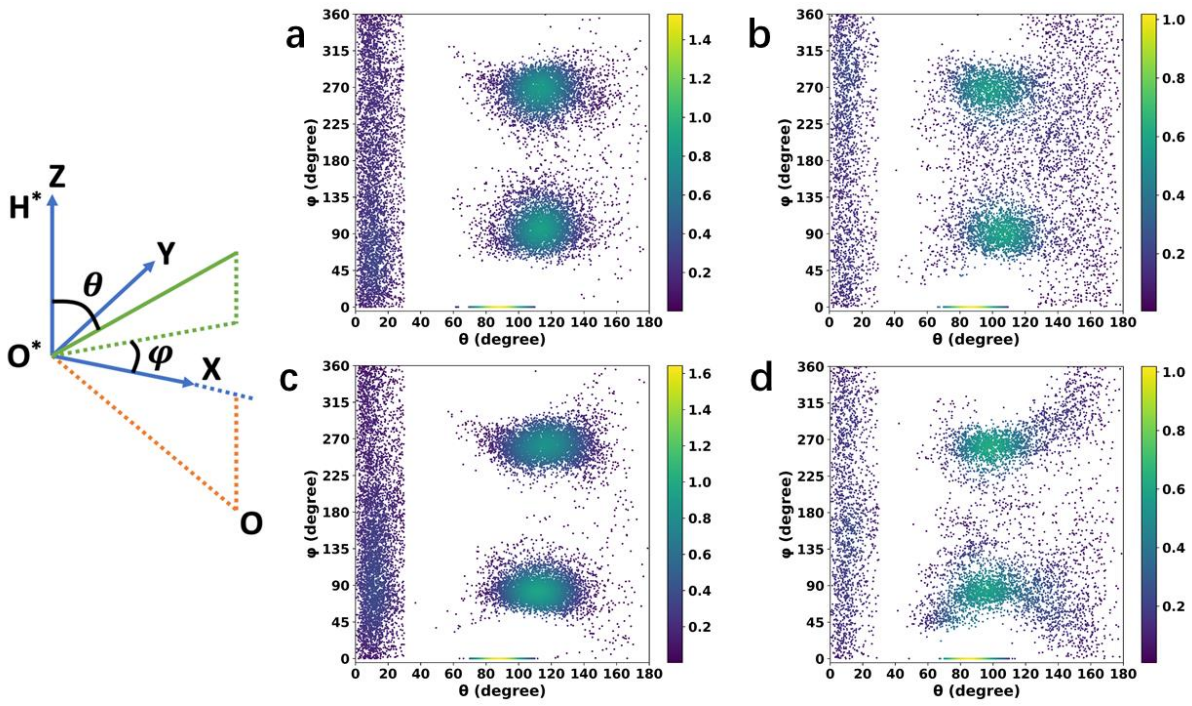

Fig. S8. Joint probability distributions *P*(θ, ϕ) computed for water oxygen atoms and water hydrogen atoms that are hydrogen-bonded or hemibonded to OH^* are depicted in (a) and (b) for OH^* in the subsurface layer with 2 and 3 hydrogen bond donors to the hemibonded O^* atom, (c) and (d) for OH^* in the interior region with 2 and 3 hydrogen bond donors to the hemibonded O^* atom, respectively. The plot is based on a Cartesian coordinate with Z axis being the vector $\vec{r}_{O^*H^*}$, and X axis being the vector on the H^*-O^*-O plane and is simultaneously perpendicular to Z axis. θ is the angle from Z axis to vector $\vec{r}_{O^*O}$ or $\vec{r}_{O^*H}$, and ϕ is the angle from X axis to the projection of vector $\vec{r}_{O^*O}$ or $\vec{r}_{O^*H}$ onto the X-Y plane.

9. The fitting of C(t)

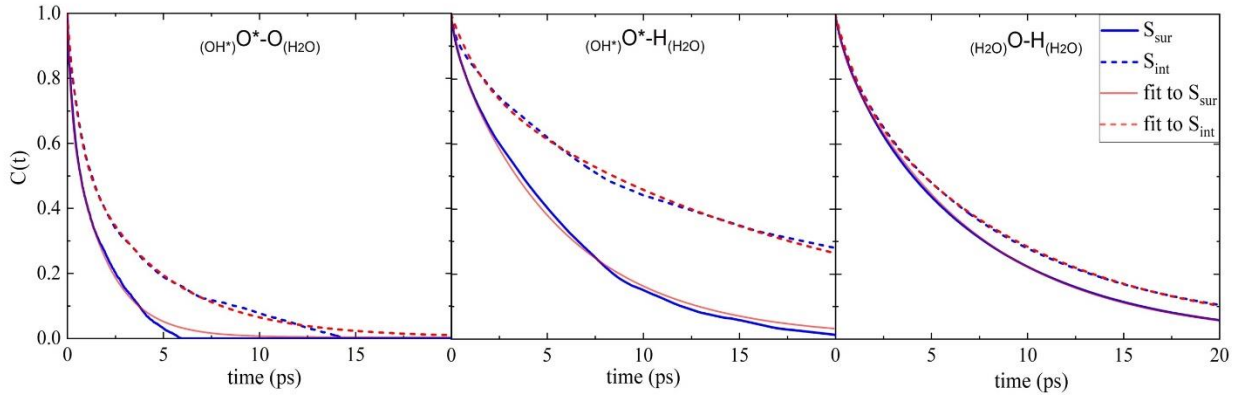

Fig. S9. The correlation function C(t) and its corresponding biexponential fit of $_{(OH^*)}O^*\text{-}O_{(H2O)}$ (hemibond), $_{(OH^*)}O^*\text{-}H_{(H2O)}$ (OH^*-involved hydrogen bonds) and $_{(H2O)}O\text{-}H_{(H2O)}$ (hydrogen bonds among water molecules only) for trajectory S_{sur} (solid curve) and S_{int} (dashed curve), respectively. For the C(t) of $_{(OH^*)}O^*\text{-}O_{(H2O)}$, the biexponential fit gives $\tau1 = 0.2$ ps, $\tau2 = 1.9$ ps for S_{sur}, and $\tau1 = 0.6$ ps, $\tau2 = 4.4$ ps for S_{int}. For the C(t) of $_{(OH^*)}O^*\text{-}H_{(H2O)}$, the biexponential fit gives $\tau1 = 0.5$ ps, $\tau2 = 5.8$ ps for S_{sur}, and $\tau1 = 1.6$ ps, $\tau2 = 17.9$ ps for S_{int}. For the C(t) of $_{(H2O)}O\text{-}H_{(H2O)}$, the biexponential fit gives $\tau1 = 0.5$ ps, $\tau2 = 7.1$ ps for S_{sur}, and $\tau1 = 1.3$ ps, $\tau2 = 9.6$ ps for S_{int}.

10. Snapshots for HT3 and HT4

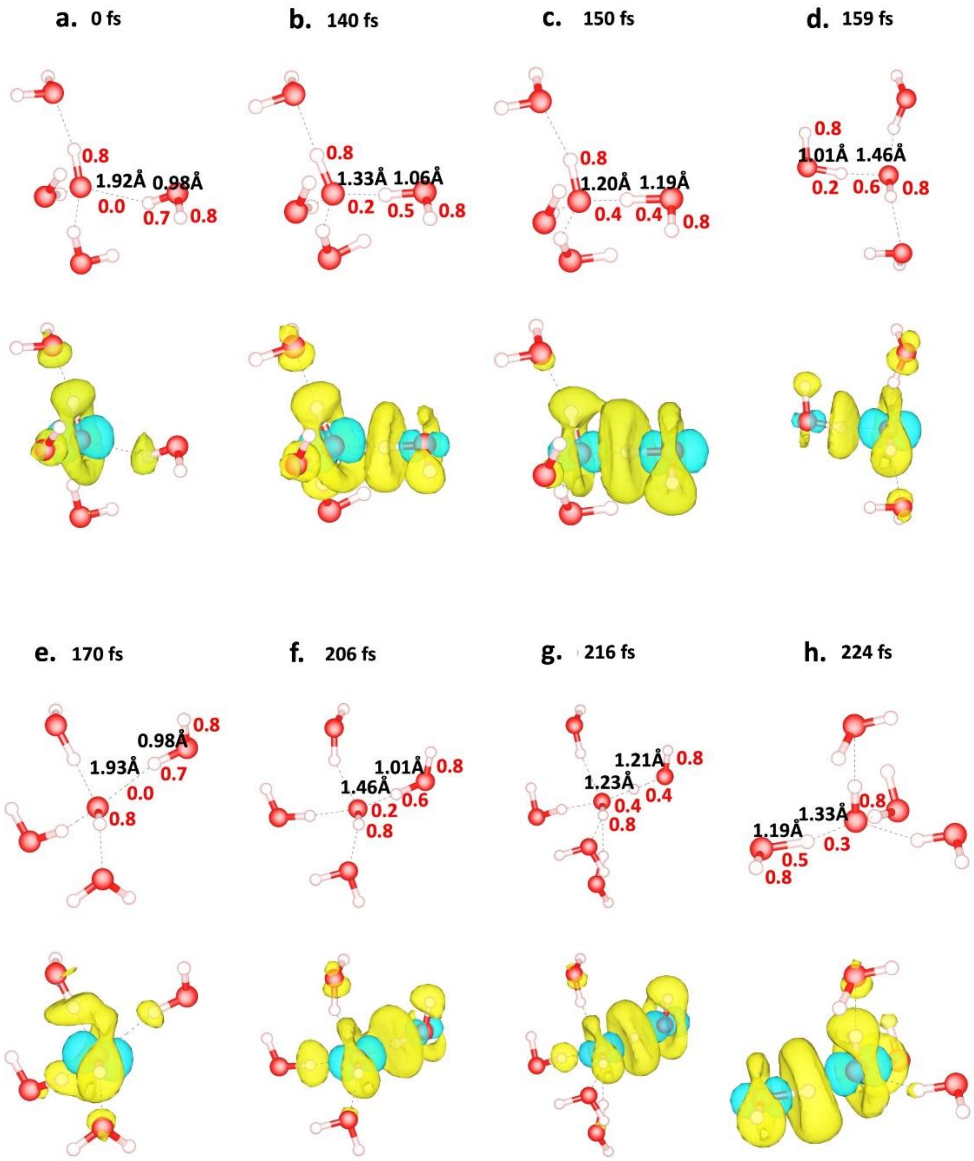

Fig. S10. The evolution of the molecular configurations and the spin density (yellow isosurfaces: +0.0005 e/Å^3; blue isosurfaces: -0.02 e/Å^3) during hydrogen transfer reactions. (a) to (d) and (e) to (h) correspond to HT3 and HT4, respectively. Bond lengths and bond orders of interest are labelled.

11. The free energy barrier of hydrogen transfer reaction

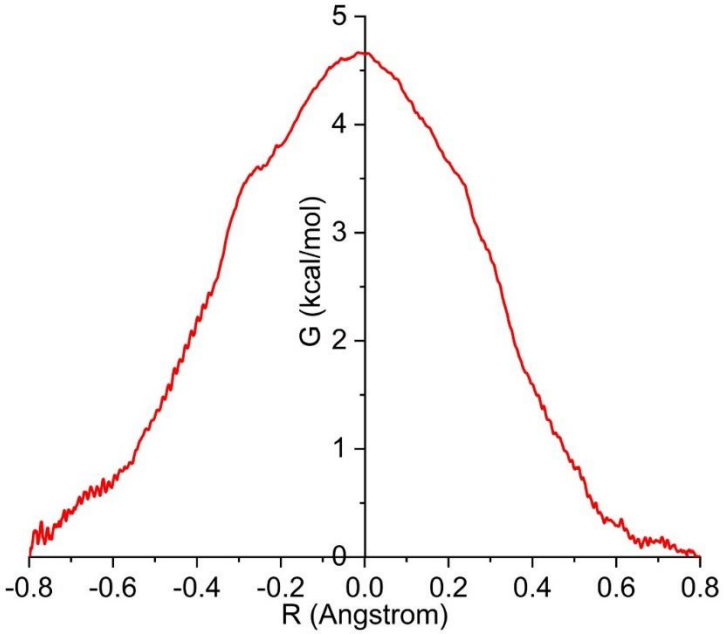

Fig. S11. The free energy barrier of the hydrogen transfer reaction between OH^* and a neighboring molecule. Slow-growth free energy simulations was used, with coordinate R being the difference between the O-H and O^*-H distances.